

THE INFLUENCE OF ELECTRIC FIELD AND TEMPERATURE ON THE ELECTRICAL CONDUCTIVITY OF POLYETHYLENE FOR POWER CABLE INSULATIONS

Lucian Viorel TARANU¹, Petru NOTINGHER², Cristina STANCU³

This paper presents a study concerning the dependence of power cables polyethylene's conductivity on temperature and electric field. In the first part the experimental results obtained on flat samples of XLPE are presented and analyzed, for an electric field between 5 and 20 kV/mm and temperatures between 30 and 70 °C. Next, the values of the conductivity are calculated using known empirical equations, and the results are compared with the experimental ones. Finally, a new equation is proposed for calculating the polyethylene's conductivity with closer results to those obtained experimentally.

Keywords: power cables insulation, polyethylene, electric field, temperature, electrical conductivity

1. Introduction

A significant part of the polyethylene manufactured today (over 10 %) is used for applications in electrical engineering [1]: as dielectrics for capacitors, insulation and jackets for power cables, for underwater cables, communication and telephone cables, in corrosive environments, low temperatures, etc. [2]. The use of polyethylene as insulation for cables is due to its low price, high processability, resistance to moisture and chemical agents, flexibility to low temperatures, low water absorption and, especially, to its excellent electrical properties. Thus, the polyethylene for power cables has a volume resistivity higher than 10^{14} Ωm, a dielectric constant and a loss factor, at 50 Hz, of 2.3 and 0.0002, respectively, and a dielectric strength higher than 15 MV/m [1].

Polyethylene (PE) is obtained by polymerization of ethylene either at high pressures (between 1000 and 2000 atm) and temperatures of 200 – 300 °C, resulting in a low-density product (LDPE), or at low pressures (50 atm) and temperatures of 20 – 70 °C, resulting in a high-density product (HDPE [1]).

Polyethylene has symmetrical and linear molecules, so it is nonpolar and thermoplastic. LDPE has a partially crystalline structure and lower mechanical

¹ Ph.D. Stud., MMAE Dept., University POLITEHNICA of Bucharest, Romania, e-mail: lv taranu@elmat.pub.ro

² Prof., MMAE Dept., University POLITEHNICA of Bucharest, Romania, e-mail: petrunot@elmat.pub.ro

³ Assoc. Prof., MMAE Dept., University POLITEHNICA of Bucharest, Romania, e-mail: cstancu@elmat.pub.ro

properties, and HDPE has a high degree of crystallinity (up to 93 %), which gives it greater hardness, higher softening point and better behavior at low temperatures (up to -40 °C). To improve the thermo-mechanical properties, polyethylene can be cross-linked: chemically (with dicumyl peroxide etc.), by electron beam irradiation or by α , β , γ radiation etc., a process by which chemical bonds between the molecular chains are made. In the case of cross-linked polyethylene (XLPE), the mobility of molecules (filiform) reduces and increases the softening temperature, working temperature (up to 90 °C) and the modulus of elasticity, whilst its dielectric properties remain practically unaffected [2].

In 1952, the first insulation for distribution cables was made from LDPE, and in 1969 also for transmission cables for voltages of 225, 400 and 500 kV. Beginning with 1970, cables with XLPE insulation were made for 138, 300 and 500 kV, with electrical stresses between 7 and 14 kV/mm (even up to 27 kV/mm) [3-4]. The existence of intense electric fields in polyethylene insulation led to the occurrence of associated phenomena, e.g. partial discharges, the accumulation of space charge and electrical and electrochemical treeing (especially water treeing), phenomena leading to ageing and degradation of the insulation.

The use of polyethylene for cable insulation and, in particular, DC cable joints, at higher electric fields and temperatures (up to 130 °C) involves the development of polyethylene compounds with reduced space charge accumulation and electrical conductivity, with less variation in regard to the temperature and the applied electric field. Thus, at the moment t after the voltage application, at the interface between two insulating layers 1 and 2 subjected to the potential difference U , a space charge of superficial density $\rho_s(t)$ is separated [5].

$$\rho_s(t) = \frac{\varepsilon_1 \sigma_2 - \varepsilon_2 \sigma_1}{\sigma_1 g_2 + \sigma_2 g_1} U \left[1 - \exp\left(-\frac{t}{\tau_{12}}\right) \right] \quad (1)$$

where g_1 and g_2 represent the thicknesses, σ_1 and σ_2 – the DC conductivities and $\varepsilon_1 = \varepsilon_0 \cdot \varepsilon_{r1}$ and $\varepsilon_2 = \varepsilon_0 \cdot \varepsilon_{r2}$ – the permittivities of the layers 1 and 2, $\varepsilon_0 = 8.85 \cdot 10^{-12}$ F/m – vacuum permittivity and τ_{12} – the charge relaxation time:

$$\tau_{12} = \frac{\varepsilon_1 g_2 + \varepsilon_2 g_1}{\sigma_1 g_2 + \sigma_2 g_1} \quad (2)$$

From equation (1) it results that the values of $\rho_s(t)$ depend on those of the conductivities and the permittivities of layers 1 and 2 and which may vary depending on the temperature and the electric field. On the other hand, increasing the electrical conductivity during the operation of cables and joints results in an increase of the active component of the current in their insulation, respectively an increase in the Joule losses in the insulation. This leads to increased insulation temperatures and hence to ageing processes and reducing their lifetime [6-8].

The electrical conduction of polymers is accomplished by electrons, holes, ions and polarons displacement under an electric field, with the electrical conductivity σ having the expression:

$$\sigma = \sum_{i=1}^n n_i q_i \mu_i \quad (3)$$

where n_i represents the concentration, q_i – the charge, μ_i – the mobility of i species of charges, and n – the number of species of charge carriers.

The conductivity values are determined by the intrinsic properties of the polymer (the length of the forbidden band gap, Fig. 1 a), but also by the nature and concentration of its defects (chemical and structural), respectively the impurities, oxidation by-products, dangling bonds, amorphous/crystalline interfaces etc. which generate new possible states in the forbidden band gap, located near defects and called, simply, traps. Carriers may encounter traps at conformational defects (chain folds) or at polar groups (in PE, carbonyl groups). Donors (electron traps) are located below the conduction band while acceptors (hole traps) are situated slightly above the valence band (Fig. 1 b) [9, 10]. The time that a carrier spends trapped in localized states depends on the depth of the trap (the energy needed to remove the carrier), temperature, electric field, etc.

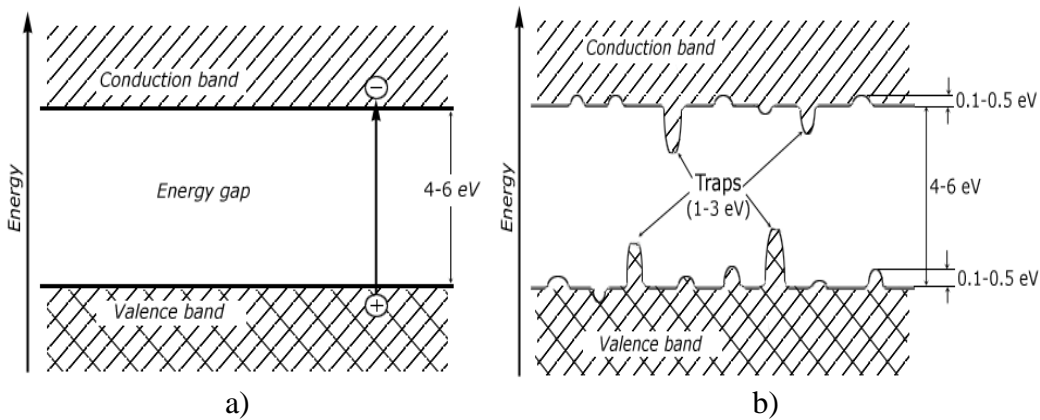


Fig. 1. Schematic representation of energy levels in a polymer:
a) ideal; b) real (with defects) [9]

In the case of polyethylene used in power cable insulations, the charge carriers are generally free electrons and holes, with low concentration and mobility (the carriers being trapped for long times), which results in low conductivity values (less than 10^{-16} S/m) [11]. The displacement of carriers takes place within the conduction (free electrons) and valence (holes) bands, the mechanisms leading to conduction and carrier transport being dependent on the electric field (among other factors). On the other hand, it is more probable that the

conduction mechanism is dominated by hopping between traps and/or the extended states (or tunneling for higher fields).

The hopping is carried out between an occupied and a nearby free state (over a potential barrier) and is due to the carrier's own (thermal) energies that increase with increasing temperatures. The probability of transition for a carrier from state i to state j (p_{ij}) can be estimated with the following equation:

$$p_{ij} = v_0 \exp\left(-\alpha_{ij}R_{ij} - \frac{\Delta w_{ij}}{kT}\right) \quad (4)$$

where v_0 represents the carrier's own oscillation frequency, α_{ij} – the tunneling coefficient, R_{ij} – the distance between the two states, Δw_{ij} – the height of the potential barrier between the two states, T – the temperature and k – Boltzmann constant [11].

Reference [12] presents a study regarding the injection, transport and trapping of the charge in LDPE, HDPE and XLPE by combined analysis of transient current measurements with space charge experiments (PEA). For low fields the authors concluded that polyethylene has ohmic behavior and probably ionic species are involved. At higher fields it is suggested a modification of the space charge limited conduction (SCLC), including heterocharges and a limited supply of charges from the electrodes, called space charge-assisted conduction.

This paper presents an experimental study on the variation of the electrical conductivity with the temperature T and the electric field E . Using the experimental results, the material parameters from 4 empirical equations are determined, and a new equation is proposed. Finally, the values of the conductivity calculated with these equations and with those determined experimentally are compared.

2. Experiments

For experiments, samples (flat disks) made from pellets of cross-linked polyethylene (XLPE) with a density of 0.92 g/cm^3 were used. The samples were realized by placing the pellets inside a stainless-steel mold and pressing (at 200 bar) in a laboratory press at ICME Bucharest. After preheating at 135°C (10 minutes at 1 bar), the pressure was increased to 100 bar (at a constant temperature) and, the temperature, at 160°C (with a speed of 2°C/min) at a constant pressure. The pressure was then increased to 200 bar (at 160°C) and then the temperature at 190°C (with 2°C/min). The 200-bar pressure was maintained at 190°C for 15 minutes, after which the sample was cooled to 35°C , maintaining the pressure at 200 bar. After their complete cooling, the samples were thermally conditioned at 50°C for 48 hours in an oven with forced air circulation. Then, their thickness was measured in 8 points and the mean thickness ($g = 0.302 - 0.307 \text{ mm}$) was determined. In order to obtain the DC conductivity, the

absorption/resorption currents were measured with a special cell (Fig. 2), in the Laboratory of Innovation Technology (LIT) of the University of Bologna.

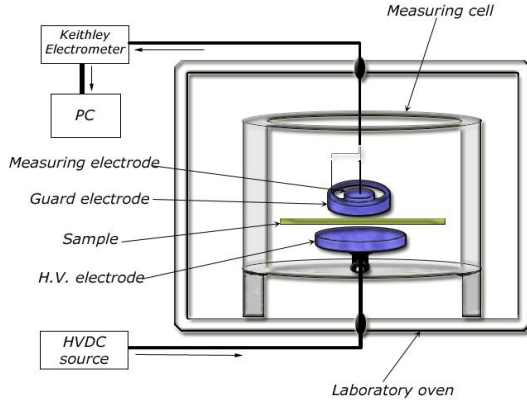


Fig 2. Setup for measuring the absorption/resorption currents

3. Results

Absorption (i_a) and resorption (i_r) currents [13] were measured (after the procedure presented in [14]) on groups of 3 samples, for one hour, at 3 temperatures (30, 50 and 70 °C) and 4 values of the electric field (5, 10, 15 and 20 kV/mm). The computation of the DC conductivity, with time, for the applied voltage U_0 ($U_0 = 1.5, 3.0, 4.5$ and 6 kV) was performed using the equation:

$$\sigma(t) = \frac{i_a(t) - i_r(t + 3600)}{U_0} \cdot \frac{g}{S}, \quad (5)$$

where $\sigma(t)$ represents the conductivity value at instant t after voltage application ($t = 0 \dots 3600$ s), and S – the surface of the measuring electrode [15]. A part of the results are presented in Figs. 3...5.

Fig. 3 shows the variations in the electrical conductivity $\sigma(t)$ with the application time of the voltage t , measured at 50 °C, for 4 values of the electric field, respectively at 5 (curves 1), 10 (curves 2), 15 (curves 3) and 20 kV/mm (curves 4). This variation is also similar for lower (30 °C) and higher (70 °C) values of the temperature. It is found that, in all cases, the conductivity decreases with the duration of the applied voltage: at the beginning very fast (at $t < 10$ s) and then slowly, stabilizing at $t > 3500$ s. This type of variation of the conductivity can be explained by the variations in the concentration and mobility of the carriers (equation (3)). Thus, after approx. 1 ns from the application of voltage, the capacitor having the measuring electrode and the high voltage electrode as the metallic plates and the sample as the dielectric (Fig. 2) is fully charged.

The absorption / resorption currents are due to the displacements of the bonded charge carriers (generating the polarization components $i_p(t)$), carriers

corresponding to the space charge components (generating the space charge currents $i_{ss}(t)$) and the carriers emitted from the electrodes (generating the conduction components $i_c(t)$ of the absorption/resorption currents).

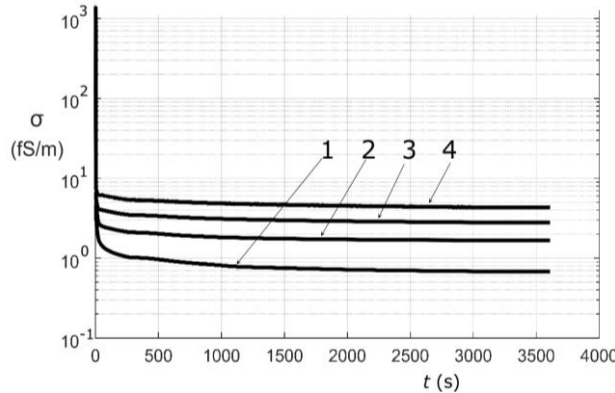


Fig. 3. Variation of electrical conductivity (σ) with voltage application time (t) at $T = 50^\circ\text{C}$ and $E = 5\text{ kV/mm}$ (1), 10 kV/mm (2), 15 kV/mm (3) and 20 kV/mm (4)

The bonded charges (associated with the electrical dipoles), although in high concentration, make very small movements that take short times. As a result, their contribution to the absorption/resorption currents is quickly cancelled over time. The space charge carriers (generated by the fracturing of molecules or by injection from the electrodes) are fixed on traps of different depths (corresponding to molecular chain ends, lattice defects etc.), and, in time, under the action of the electric field, move on shorter or longer distances, until they fall in another trap or are captured by the electrodes. As a result, the concentration and therefore, the contribution of space charge carriers to the absorption/resorption currents, decreases in time (but slower than in the case of bonded charges).

Only a part of the carriers emitted by the electrodes or generated by ionizing collisions of the molecules of material pass the entire thickness of the sample, generates the conduction current i_c (considered constant and characterizing the intrinsic conductivity of the material). In our experiments it was considered that, after 3600 s, the contribution of the space charges is negligible compared to the contribution of the carriers corresponding to the conduction current and, as such, can be considered that, after 3600 s, the conductivity remains constant.

Increasing the electric field (from 5 to 20 kV/mm) and the temperature (from 30 to 70 °C) leads to an increase in the electrical conductivity values (Figs. 3-5). Thus, at $T = 70^\circ\text{C}$, the increase of the electric field from 5 to 20 kV/mm determined an increase in the conductivity values of approx. 4 times (Fig. 4), and in the case of 10 kV/mm, the temperature rise from 30 to 70 °C led to an increase of conductivity values of approx. 2.5 times (Fig. 5). The increases are due, on one

hand, to the increase of the charge concentration and, on the other hand to the increase of their mobility.

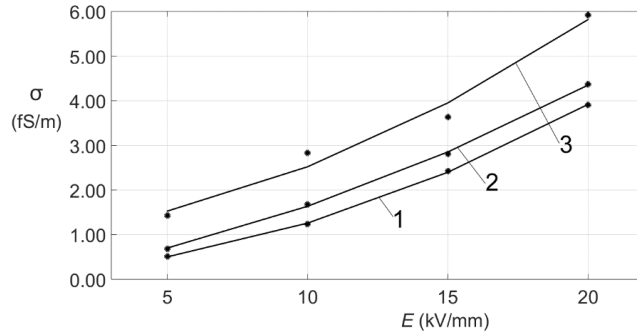


Fig. 4. Variation of electrical conductivity (σ) with electric field (E), at $T = 30$ °C (1), 50 °C (2) and 70 °C (3) ($t = 3600$ s)

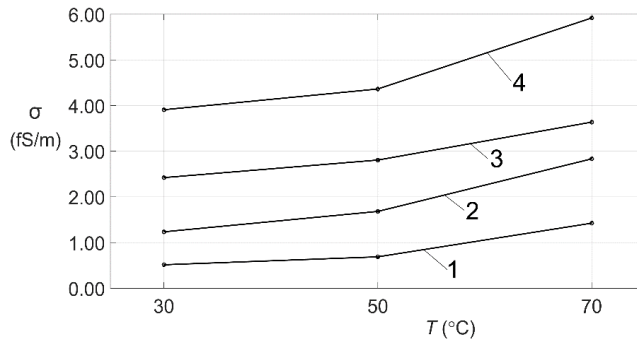


Fig. 5. Variation of electrical conductivity (σ) with temperature (T), at $E = 5$ kV/mm (1), 10 kV/mm (2), 15 kV/mm (3) and 20 kV/mm (4) ($t = 3600$ s)

The increase in concentration is mainly due to the rise in the probability of detrapping of the charges due to the reduction of the heights of potential barriers related to traps in which they are trapped by increasing the electric field and the temperature, whereas the increase in the mobility is mainly related to the increase of the diffusion coefficient of the ionic carriers with the rise in temperature. In general, the more significant increases of the conductivity with E are observed at higher temperatures (70 °C) (Figs. 4-5).

4. Computation of the electrical conductivity

In Figs. 4-5 the variation curves of electrical conductivity with temperature and electric field resulted from a relative reduced number of experiments were presented. These allow obtaining some empirical equations of the XLPE conductivity for other temperatures and fields than those used in experiments. Other similar equations, considering $\sigma = f(T)$ [2], $\sigma = f(E)$ [16] or

$\sigma = f(T, E)$ [17-24] are known, the most used being (6) [17-20], (7), (8) [21-22] and (9) [23-24]:

$$\sigma(E, T) = A \exp\left(-\frac{E_a}{kT}\right) \frac{\sinh((aT + b)E)}{E} \quad (6)$$

$$\sigma(E, T) = A \exp\left(-\frac{E_a}{kT}\right) \frac{\sinh((aT + b)E^{1/2})}{E} \quad (7)$$

$$\sigma(E, T) = A \exp\left(-\frac{E_a}{kT}\right) \frac{\sinh((aT + b)E^{1/3})}{E} \quad (8)$$

$$\sigma(E, T) = A \exp\left(-\frac{E_a}{kT}\right) \sinh((aT + b)E^\alpha) \quad (9)$$

where E_a is the activation energy, A , a , b and α – material constants, k – Boltzmann constant and E – electric field value divided per unit (dimensionless).

Replacing the experimental values of the conductivity presented in Table 1 in the eq. (6) – (9), 4 (for equations (6)...(8)), respectively 5 equations systems (for (9)) were obtained. The unknown values of A , E_a , a , b and α , were numerically obtained using the Matlab software, with the *fsolve* function from the *Optimization Toolbox* package. For equations (6) – (8), values 1–4 of electrical conductivity were used at $T < 50$ °C – and 3–4, 6–7 at $T > 50$ °C (Table 1).

Numerical values of A , E_a , a , b and α corresponding to the empirical equations (6) – (9) are presented in Table 2. Using these values, the variation curves of conductivity $\sigma = f(T, E)$, for values of the electric field between 5 and 20 kV/mm and temperatures between 30 and 70 °C, were drawn. The variation curves obtained are presented only for $T = 70$ °C in Fig. 6 but are also similar for 30 and 50 °C.

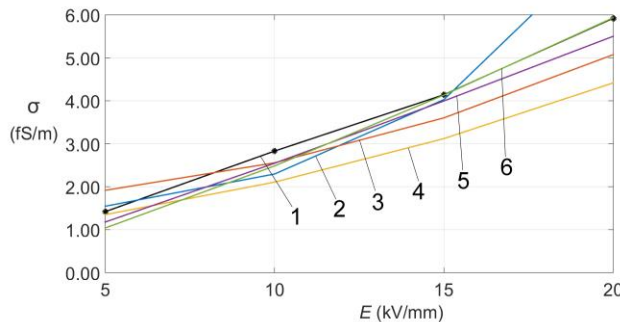


Fig. 6. Variation of electrical conductivity (σ) with electric field (E) determined experimentally (curve 1) and calculated with (6) (curve 2), (7) (curve 3), (8) (curve 4), (9) (curve 5) and (10) (curve 6) ($T = 70$ °C)

Analyzing the results presented in Fig. 6, it is found that there are differences (more or less) between the values of the conductivities calculated with equations (6) – (9) and those experimentally determined, according to the

equation used and the temperature and electric field values. These differences can exceed 53 % - for equation (6), 63 % - for equation (7), 33 % - for equation (8) and 55 % - for equation (9).

To obtain values closer to the experimental ones, a new empirical equation for the electrical conductivity $\sigma(E, T)$ is proposed:

$$\sigma(E, T) = A \exp\left(-\frac{E_a}{kT}\right) \frac{\sinh((aT + b)\ln E)}{E} \quad (10)$$

The new values of A , E_a , a and b are presented in Table 2 (equation (10)), and the variation curves of the conductivity with E and T in Fig. 6.

Table 1
Values of electrical conductivity σ of XLPE samples for different temperatures (T) and electric fields (E)

No.	T (°C)	E (kV/mm)	σ (fS/m)
1	30	5	0.513
2	30	20	3.910
3	50	5	0.687
4	50	20	4.460
5	50	10	1.680
6	70	5	1.420
7	70	20	5.920
8	70	10	2.830

Table 2
Values of A , E_a , a , b and α related to equations (6) – (10)

Eq.	T (°C)	A (S/m)	E_a (eV)	a (1/K)	b (-)	α (-)
(6)	≤ 50	0.5	0.5347	$-2.8746 \cdot 10^{-9}$	$1.147 \cdot 10^{-6}$	-
	≥ 50			$-2.8535 \cdot 10^{-9}$	$1.1688 \cdot 10^{-6}$	
(7)	≤ 50	0.1259	0.5336	$-1.2673 \cdot 10^{-5}$	0.0054	-
	≥ 50					
(8)	≤ 50	0.0132	0.5374	$-2.1043 \cdot 10^{-4}$	0.0978	-
	≥ 50					
(9)	≤ 50	25	0.55	$-1.543 \cdot 10^{-16}$	$5.1195 \cdot 10^{-14}$	0.045
	≥ 50			$-1.3696 \cdot 10^{-17}$	$4.9247 \cdot 10^{-15}$	0.111
(10)	≤ 50	$9.5234 \cdot 10^{-16}$	0.55	-0.0034	3.406	-
	≥ 50			-0.0023675	3.0685	

It can be seen that the values of the electrical conductivity calculated with (10) (curve 6, Fig. 6) are very close to the ones experimentally determined (curve 1, Fig. 6).

The relative differences between the calculated $\sigma_c(E, T)$ and experimental $\sigma_m(E, T)$ values of the conductivity, determined with the equation:

$$\varepsilon_{rel} = \frac{|\sigma_c(E, T) - \sigma_m(E, T)|}{\sigma_m(E, T)} \cdot 100 \quad [\%] \quad (11)$$

have average values below 10 %, for all the temperatures. The maximum value of the relative difference (26.7 %) was obtained for $E = 5$ kV/mm and $T = 70$ °C, and the minimum one (0.2 %) – for $E = 15$ and 20 kV/mm and $T = 70$ °C. Consequently, it can be said that for values of the electric field between 5 and 20 kV/mm, the calculated values of the conductivity using equation (10) are closest to the experimental ones.

The quantities A , E_a , a and b , involved in equation (10) were determined using the conductivity values experimentally determined for fields between 5 and 20 kV/mm. As, in the case of cables and joints insulation, values of E can be lower than 5 kV/mm or higher than 20 kV/mm, the conductivity values were calculated also, for fields between 1 and 5 kV/mm and 20 and 40 kV/mm. The experimental conductivity values were obtained by prolonging the experimental curves (Fig. 7) using interpolating functions associated with the experimental data points (determined with the MATLAB software).

For electric field values lower than 5 kV/mm, the differences between the calculated and experimental values are higher than those corresponding to fields between 5 and 20 kV/mm. Instead, for $E > 20$ kV/mm these differences are lower, reaching up to 0.5 % for $E = 40$ kV/mm and $T = 30$ °C (Fig. 7, curves 1 and 2). Consequently, equation (10) can be used for any field lower than 40 kV/mm. Certainly, for a more accurate verification, new tests should be done, at fields lower than 5 kV/mm and higher than 20 kV/mm.

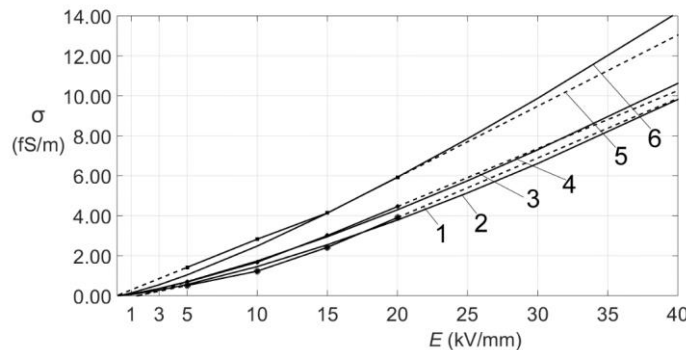


Fig. 7. Variation of electrical conductivity σ with electric field E experimental (curves 1, 3 and 5) and calculated ones (curves 2, 4 and 6) with equation (10) at $T = 30$ °C (curves 1, 2), 50 °C (curves 3, 4) and 70 °C (curves 5, 6)

5. Conclusions

Experiments performed on cross-linked polyethylene samples show that the electrical conductivity values are strongly influenced by those of the electric field and temperature.

In the case of tested XLPE samples, empirical equations proposed in literature for electric conductivity of polymers lead - for fields between 5 and 20 kV/mm and temperatures between 30 and 70 °C - to important errors (even above 60 %).

The new empirical equation proposed in the paper allows the electrical conductivity values calculation with higher accuracy and for larger intervals of E , the average differences between the calculated and experimental values being under 10 %.

Acknowledgements

The authors express their acknowledgement to ICME ECAB Bucharest for technical support regarding the samples manufacturing and to the Laboratory of Innovation Technology (LIT) of the University of Bologna for the conductivity measurement setup and assistance.

R E F E R E N C E S

- [1]. *R. Bartnikas, K.D.Srivastava*, Power and Communication Cables. Theory and Applications, IEEE Press, New York, 2000.
- [2]. *P.V.Notingher*, Materiale pentru Electrotehnica (Materials for Electrotechnics), Vol. 2, Politehnica Press, 2005.
- [3]. *L.Dechamps, R. Michel, L. Lapers*, Development in France of High Voltage Cables with Synthetic insulation, CIGRE, Paris, 1980, report 21-06.
- [4]. *U. Amerpoh, H. Koberh, C.van Hove, H. Schadlich, G. Ziemeck*, Development of Polyethylene Insulated Cables for 220 kV and higher Voltages, CIGRE, Paris, 1980, Report 21-11.I.
- [5]. *C. Stancu, P.V. Notingher, P. Notingher, M. Lungulescu*, Space Charge and Electric Field in Thermally Aged Multilayer Joints Model, IEEE Transactions on Dielectrics and Electrical Insulation, Vol. 23, No. 2, 2016, pp.633-644.
- [6]. *M.G. Ploceanu, P.V. Notingher, C. Stancu, S. Grigorescu*, Underground power cable insulation electrical lifetime estimation methods, Scientific Bulletin of University POLITEHNICA of Bucharest, Series C: Electrical Engineering and Computer Science, Vol. 75, Iss. 1, 2013, pp. 233-238, ISSN 1454-234x (B+).
- [7]. *C. Rusu-Zagar, P.V. Notingher, S. Busoi, M. Lungulescu, G. Rusu-Zagar*, Rapid Estimation of Lifetime and Residual Lifetime for Silicone Rubber Cable Insulation, UPB Scientific Bulletin, Series C, Vol. 79, Iss. 1, 2017, pp.181-196, ISSN 2286-3540.
- [8]. *L.A. Dissado, J.e. Fothergill*, Electrical Degradation and Breakdown in Polymers, IEE P. Peregrinus, London, 1992.
- [9]. *B. Hilczer, J. Malecki*, Electrets, Elsevier, Warsaw, 1986.
- [10]. *G. Blaise*, “Charge localization and transport in disordered dielectric materials”, J. Electrostatics, vol. 50, 2001, pp. 69-89.

[11]. *M.C. Lanca*, Electrical Ageing Studies of Polymeric Insulation for Power Cables, PhD Thesis, Universida de Nova de Lisboa, Lisbon, 2002.

[12]. *G.C. Montanari, G. Mazzanti, F. Palmieri, A. Motori, G. Perego, S. Serra*, Space-charge trapping and conduction in LDPE, HDPE and XLPE, *J. Phys. D: Appl. Phys.*, vol. 34, 2001, pp. 2902-2911.

[13]. *C. Stancu, P. V. Notingher*, Influence of the Surface Defects on the Absorption/Resorption Currents in Polyethylene Insulations, *Scientific Bulletin of University POLITEHNICA of Bucharest, Series C: Electrical Engineering and Computer Science*, vol. 72, Iss. 2, 2010, pp. 161 – 170.

[14]. *C. Stancu*, Méthodes d'estimation de l'état de vieillissement des câbles d'énergie, Editions universitaires européennes, LAMBERT Academic Publishing, Riga, 2018.

[15]. *C. Stancu, P.V. Notingher, P. Notingher jr.*, Computation of the Electric Field in Aged Underground Medium Voltage Cable Insulation, *IEEE Transactions on Dielectrics and Electrical Insulation*, Vol. 20, Issue 5, 2013, pp. 1530-1539.

[16]. *C. Stancu, P.V. Notingher, P.P. Notingher, M. Lungulescu*, Space Charge and Electric Field in Thermally Aged Multilayer Joints Model, *IEEE Transactions on Dielectrics and Electrical Engineering*, Vol. 23, No. 2, 2016, pp. 633-644.

[17]. *S. Boggs, D. H. Damon, J. Hjerrild, J. T. Holboll, and M. Henriksen*, “Effect of insulation properties on the field grading of solid dielectric DC cable”, *IEEE Trans. Power Deliv.*, vol. 16, no. 4, 2001, pp. 456–461.

[18]. *C. Stancu, P. V. Notingher, L. M. Dumitran, L. Taranu, A. Constantin, and A. Cernat*, “Electric field distribution in dual dielectric DC cable joints”, in 2016 IEEE International Conference on Dielectrics (ICD), 2016, pp. 402–405.

[19]. *N. Adi, G. Teyssedre, T. T. N. Vu, and N. I. Sinisuka*, “DC field distribution in XLPE-insulated DC model cable with polarity inversion and thermal gradient”, in 2016 IEEE International Conference on High Voltage Engineering and Application (ICHVE), 2016, pp. 1–4.

[20]. *Z. Xu, W. Choo, and G. Chen*, “DC electric field distribution in planar dielectric in the presence of space charge”, in 2007 IEEE International Conference on Solid Dielectrics, 2007, pp. 514–517.

[21]. *O. L. Hestad, F. Mauseth, and R. H. Kyte*, “Electrical conductivity of medium voltage XLPE insulated cables”, in 2012 IEEE International Symposium on Electrical Insulation, 2012, pp. 376–380.

[22]. *G. Jiang, J. Kuang, and S. Boggs*, “Evaluation of high field conduction models of polymeric dielectrics”, in 2000 Annual Report Conference on Electrical Insulation and Dielectric Phenomena (Cat. No.00CH37132), vol. 1, pp. 187–190.

[23]. *T. N. Vu, G. Teyssedre, B. Vissouvanadin, S. Roy, and C. Laurent*, “Correlating conductivity and space charge measurements in multi-dielectrics under various electrical and thermal stresses”, *IEEE Trans. Dielectr. Electr. Insul.*, vol. 22, no. 1, 2015, pp. 117–127.

[24]. *T. T. N. Vu, G. Teyssedre, S. Le Roy, and C. Laurent*, “Maxwell–Wagner Effect in Multi-Layered Dielectrics: Interfacial Charge Measurement and Modelling”, *Technologies*, vol. 5, no. 4, 2017, pp. 27-42.